Heat flux in binary gas mixtures confined between two parallel plates via moment equations

Cite as: AIP Conference Proceedings **2132**, 120003 (2019); https://doi.org/10.1063/1.5119616
Published Online: 05 August 2019

Vinay Kumar Gupta, and Manuel Torrilhon

Heat Flux in Binary Gas Mixtures Confined between Two Parallel Plates via Moment Equations

Vinay Kumar Gupta[1,2,a),b)] and Manuel Torrilhon[3,c)]

[1] *Mathematics Institute, University of Warwick, Coventry CV4 7AL, UK.*
[2] *SRM Research Institute and Department of Mathematics, SRM Institute of Science and Technology, Chennai 603203, India.*
[3] *Center for Computational Engineering Science, Department of Mathematics, RWTH Aachen University, Schinkelstr. 2, D-52062 Aachen, Germany*

[a)] Corresponding author: vinay.gupta@warwick.ac.uk
[b)] URL: https://warwick.ac.uk/fac/sci/maths/people/staff/gupta/
[c)] mt@mathcces.rwth-aachen.de

Abstract. The steady heat transfer problem in two-component gas mixtures of noble (monatomic) gases confined between two infinite parallel plates having different temperatures has been investigated with the Grad 13- and 26-moment equations for Maxwell molecules as well as for hard-sphere molecules. The heat flux normal to the plates is computed via the aforementioned models for three gas mixtures, namely neon–argon, helium–argon and helium–xenon, for different mole fraction ratios. The heat flux profiles computed through the Grad moment equations in this work turn out to be in reasonably good agreement with those obtained through the discrete velocity method in [1].

INTRODUCTION

It is well-established that the classical fluid dynamics models, e.g., the Euler equations or Navier–Stokes–Fourier (NSF) equations, are inadequate for gas flows in the transition regime [2–7]—commonly encountered in rarefied situations, for instance in complex conduits of micro- and nano-devices and in reentry flows. Processes in rarefied gases can also be described by the Boltzmann equation, which is solved for the velocity distribution function, the fundamental quantity in kinetic theory of gases. Although, the Boltzmann equation is capable of describing processes in all flow regimes ranging from hydrodynamic to free-flight regimes (i.e., for all values of the Knudsen number, which is defined as ratio of mean free path to a macroscopic length scale pertaining to the problem), the direct solutions of the Boltzmann equation are forbiddingly time expensive, particularly in the transition regime [4, 6].

To overcome these problems and aiming to reduce the high dimensionality of the velocity distribution function in the Boltzmann equation to a low-dimensional continuum model, processes in rarefied gases can be described, alternatively, through macroscopic models, which consist of the transport equations for physical quantities, such as density, velocity, temperature, stress and heat flux. These quantities are related to the velocity distribution function as its *moments*; and consequently, the transport equations in a macroscopic model are, in general, referred to as the *moment equations*.

Moment equations obtained through the Grad moment method [8] and their variants, e.g. regularized moment equations [6, 9–11], globally hyperbolic regularized moment equations [12, 13], quadrature-based moment equations [14] have proven to be quite successful in describing several non-equilibrium phenomena in rarefied single-component monatomic gases efficiently and accurately, see e.g. [6, 11, 15–21] and references therein. Motivated from the success of moment method for rarefied single-component monatomic gases, the present authors, in the last few years, have extended the Grad moment method to multi-component monatomic gas mixtures interacting with Maxwell [22] and hard-sphere [23] interaction potentials, and derived the regularized moment equations for two-component monatomic gas mixtures of Maxwell molecules [24]. Recently, the method has also been extended to single-component rarefied granular gases of hard spheres [25–27]. It is worth to note that the computation of full

31st International Symposium on Rarefied Gas Dynamics
AIP Conf. Proc. 2132, 120003-1–120003-12; https://doi.org/10.1063/1.5119616
Published by AIP Publishing. 978-0-7354-1874-5/$30.00

nonlinear production terms—the terms arising from the Boltzmann collision operator—associated with the moment equations derived in these works is not easy, and the present authors have also developed an automated way to compute them using computer algebra software MATHEMATICA®, see [23, 28–30] for its details and [31] for the source code.

In this paper, Grad moment equations for multi-component monatomic gas mixtures derived in References [22, 23] are employed to investigate the problem of steady-state heat transfer in a gas mixture confined between two infinite parallel plates having different temperatures. This is a classical problem in rarefied gas dynamics, since the steady heat flux is one of the simplest examples of non-equilibrium through which different methods and approaches can be examined and compared. The problem has been studied extensively by several researchers in the context of single-component monatomic gases, see e.g., [32–38] and the references cited in [36, 37]. However, the same problem in the context of gaseous mixtures has certainly received less attention and there exists only a handful number of papers in the literature on this problem in the context of gaseous mixtures [1, 22, 39–45]. To the best of authors' knowledge, the first paper on heat transfer between parallel plates in the context of binary gas mixtures goes back to 1970s [39]. More recently, Kosuge, Aoki, and Takata [40] have investigated the non-linear heat transfer based on the numerical solution of the Boltzmann equations. Reference [41] studies the problem using the linearized McCormack kinetic model [46] of the Boltzmann equations. Reference [1] also reports the results based on McCormack kinetic model, but uses two interaction potentials, namely, the hard-sphere interaction potential and the so-called realistic potential. References [42, 43] study the problem on the basis of linearized Boltzmann equations for binary gas mixtures with hard-sphere interaction potential. Reference [44] studies the problem via linearized extended thermodynamics with 13 moments for each constituent in a binary gas mixture. Reference [45] reports the results based on the DSMC method with an implementation of the *ab initio* potential. The present authors have also studied this problem with Grad 26-moment (G26) equations for each component in a binary gas mixtures of Maxwell molecules (MM) in [22].

In this paper, we investigate this problem for two-component gas mixtures with the systems of Grad 2×13-moment (2×G13) equations as well as Grad 2×26-moment (2×G26) equations, both for MM and hard spheres (HS) derived in [22, 23]. A part of it (the same problem with 2×G26 equations for MM) has already been presented in [22]. Notwithstanding, we shall include those results here as well for comparison purpose.

PROBLEM DESCRIPTION

Let us consider a gas mixture of two monatomic gases α and β confined between two infinite parallel plates placed at $x = \pm L/2$ and let the temperature of the left plate (at $x = -L/2$) and that of the right plate (at $x = L/2$) be $T_w^{\mathrm{L}} = T_0 + \varepsilon \Delta \tilde{T}_w/2$ and $T_w^{\mathrm{R}} = T_0 - \varepsilon \Delta \tilde{T}_w/2$, respectively. The schematic of the problem is shown in Figure 1. Owing to the temperature difference between the plates, the heat transfer takes place in the normal direction to the plates, i.e., in the x-direction, and therefore, the y-axis in Figure 1 is shown just for illustration purpose. The temperature difference between the plates $\varepsilon \Delta \tilde{T}_w$ is taken very small in comparison to T_0 (a reference temperature) so that the linearized equations and linearized boundary conditions are sufficient for the description of the process.

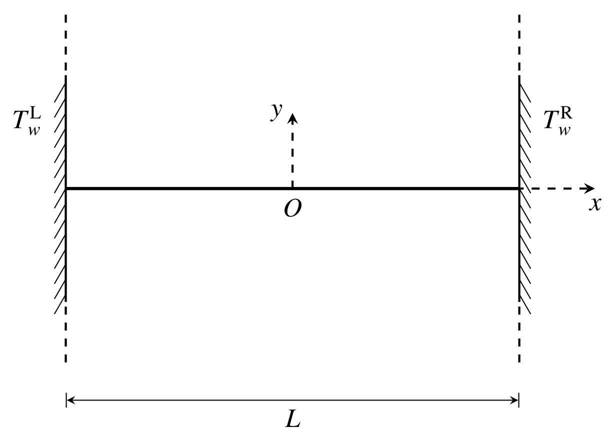

FIGURE 1. Schematic of the heat transfer problem in a binary gas mixture confined between infinite parallel plates having different temperatures; y-axis is included just for illustration.

GRAD MOMENT SYSTEMS AND BOUNDARY CONDITIONS

The problem is studied with the Grad moment equations for a multi-component gas mixture, which are derived from the Boltzmann equation for each component. The detailed derivation of the Grad moment equations for a N-component gas mixture can be found in [22, 23]. Here, we present the Grad moment equations for a monatomic two-component gas mixture directly for the sake of succinctness.

Grad moment equations

The G26 equations—without any external force—for the component α in a binary mixture of monatomic gases α and β read [22, 23]

$$\frac{\partial \rho_\alpha}{\partial t} + \frac{\partial(\rho_\alpha v_i)}{\partial x_i} + \frac{\partial(\rho_\alpha u_i^{(\alpha)})}{\partial x_i} = 0, \tag{1}$$

$$\frac{\partial(\rho_\alpha u_i^{(\alpha)})}{\partial t} + \frac{\partial \sigma_{ij}^{(\alpha)}}{\partial x_j} + \frac{\partial(\rho_\alpha \theta_\alpha)}{\partial x_i} + \frac{\partial(\rho_\alpha u_i^{(\alpha)} v_j)}{\partial x_j} + \rho_\alpha u_j^{(\alpha)} \frac{\partial v_i}{\partial x_j} + \rho_\alpha \frac{\mathrm{D} v_i}{\mathrm{D} t} = \mathcal{P}_i^{0(\alpha)}, \tag{2}$$

$$\frac{3}{2}\frac{\partial(\rho_\alpha \theta_\alpha)}{\partial t} + \frac{3}{2}\frac{\partial(\rho_\alpha \theta_\alpha v_i)}{\partial x_i} + \frac{\partial q_i^{(\alpha)}}{\partial x_i} + \sigma_{ij}^{(\alpha)} \frac{\partial v_i}{\partial x_j} + \rho_\alpha \theta_\alpha \frac{\partial v_i}{\partial x_i} + \rho_\alpha u_i^{(\alpha)} \frac{\mathrm{D} v_i}{\mathrm{D} t} = \frac{1}{2}\mathcal{P}^{1(\alpha)}, \tag{3}$$

$$\frac{\partial \sigma_{ij}^{(\alpha)}}{\partial t} + \frac{\partial(\sigma_{ij}^{(\alpha)} v_k)}{\partial x_k} + \frac{\partial m_{ijk}^{(\alpha)}}{\partial x_k} + \frac{4}{5}\frac{\partial q_{\langle i}^{(\alpha)}}{\partial x_{j\rangle}} + 2\sigma_{k\langle i}^{(\alpha)} \frac{\partial v_{j\rangle}}{\partial x_k} + 2\rho_\alpha \theta_\alpha \frac{\partial v_{\langle i}}{\partial x_{j\rangle}} + 2\rho_\alpha u_{\langle i}^{(\alpha)} \frac{\mathrm{D} v_{j\rangle}}{\mathrm{D} t} = \mathcal{P}_{ij}^{0(\alpha)}, \tag{4}$$

$$\begin{aligned}
&\frac{\partial q_i^{(\alpha)}}{\partial t} + \frac{\partial(q_i^{(\alpha)} v_j)}{\partial x_j} + \frac{1}{2}\frac{\partial R_{ij}^{(\alpha)}}{\partial x_j} + \frac{7}{2}\theta_\alpha \frac{\partial \sigma_{ij}^{(\alpha)}}{\partial x_j} + \frac{7}{2}\sigma_{ij}^{(\alpha)} \frac{\partial \theta_\alpha}{\partial x_j} + \frac{1}{6}\frac{\partial \Delta_\alpha}{\partial x_i} + \frac{5}{2}\frac{\partial(\rho_\alpha \theta_\alpha^2)}{\partial x_i} + m_{ijk}^{(\alpha)} \frac{\partial v_j}{\partial x_k} \\
&\quad + \frac{2}{5} q_i^{(\alpha)} \frac{\partial v_j}{\partial x_j} + \frac{7}{5} q_j^{(\alpha)} \frac{\partial v_i}{\partial x_j} + \frac{2}{5} q_j^{(\alpha)} \frac{\partial v_j}{\partial x_i} + \left(\sigma_{ij}^{(\alpha)} + \frac{5}{2}\rho_\alpha \theta_\alpha \delta_{ij}\right) \frac{\mathrm{D} v_j}{\mathrm{D} t} = \frac{1}{2}\mathcal{P}_i^{1(\alpha)},
\end{aligned} \tag{5}$$

$$\frac{\partial m_{ijk}^{(\alpha)}}{\partial t} + \frac{\partial(m_{ijk}^{(\alpha)} v_l)}{\partial x_l} + \frac{3}{7}\frac{\partial R_{\langle ij}^{(\alpha)}}{\partial x_{k\rangle}} + 3\theta_\alpha \frac{\partial \sigma_{\langle ij}^{(\alpha)}}{\partial x_{k\rangle}} + 3\sigma_{\langle ij}^{(\alpha)} \frac{\partial \theta_\alpha}{\partial x_{k\rangle}} + 3 m_{l\langle ij}^{(\alpha)} \frac{\partial v_{k\rangle}}{\partial x_l} + \frac{12}{5} q_{\langle i}^{(\alpha)} \frac{\partial v_{k\rangle}}{\partial x_j} + 3\sigma_{\langle ij}^{(\alpha)} \frac{\mathrm{D} v_{k\rangle}}{\mathrm{D} t} = \mathcal{P}_{ijk}^{0(\alpha)}, \tag{6}$$

$$\begin{aligned}
&\frac{\partial R_{ij}^{(\alpha)}}{\partial t} + \frac{\partial(R_{ij}^{(\alpha)} v_k)}{\partial x_k} + 2\theta_\alpha \frac{\partial m_{ijk}^{(\alpha)}}{\partial x_k} + 9 m_{ijk}^{(\alpha)} \frac{\partial \theta_\alpha}{\partial x_k} + \frac{28}{5}\theta_\alpha \frac{\partial q_{\langle i}^{(\alpha)}}{\partial x_{j\rangle}} + \frac{56}{5} q_{\langle i}^{(\alpha)} \frac{\partial \theta_\alpha}{\partial x_{j\rangle}} - 14\rho_\alpha \theta_\alpha^2 \frac{\partial u_{\langle i}^{(\alpha)}}{\partial x_{j\rangle}} - 14\theta_\alpha^2 u_{\langle i}^{(\alpha)} \frac{\partial \rho_\alpha}{\partial x_{j\rangle}} \\
&\quad - 28\rho_\alpha \theta_\alpha u_{\langle i}^{(\alpha)} \frac{\partial \theta_\alpha}{\partial x_{j\rangle}} + 4\theta_\alpha \sigma_{k\langle i}^{(\alpha)} \frac{\partial v_k}{\partial x_{j\rangle}} + 4\theta_\alpha \sigma_{k\langle i}^{(\alpha)} \frac{\partial v_{j\rangle}}{\partial x_k} - \frac{8}{3}\theta_\alpha \sigma_{ij}^{(\alpha)} \frac{\partial v_k}{\partial x_k} - \frac{14}{3}\frac{1}{\rho_\alpha}\sigma_{ij}^{(\alpha)} \frac{\partial q_k^{(\alpha)}}{\partial x_k} \\
&\quad - \frac{14}{3}\frac{1}{\rho_\alpha}\sigma_{ij}^{(\alpha)} \sigma_{kl}^{(\alpha)} \frac{\partial v_k}{\partial x_l} + 7\theta_\alpha \sigma_{ij}^{(\alpha)} \frac{\partial u_k^{(\alpha)}}{\partial x_k} + 7\frac{1}{\rho_\alpha}\theta_\alpha u_k^{(\alpha)} \sigma_{ij}^{(\alpha)} \frac{\partial \rho_\alpha}{\partial x_k} + \frac{6}{7} R_{\langle ij}^{(\alpha)} \frac{\partial v_{k\rangle}}{\partial x_k} + \frac{4}{5} R_{k\langle i}^{(\alpha)} \frac{\partial v_k}{\partial x_{j\rangle}} \\
&\quad + 2 R_{k\langle i}^{(\alpha)} \frac{\partial v_{j\rangle}}{\partial x_k} + \frac{14}{15}\Delta_\alpha \frac{\partial v_{\langle i}}{\partial x_{j\rangle}} + 2 m_{ijk}^{(\alpha)} \frac{\mathrm{D} v_k}{\mathrm{D} t} + \frac{28}{5}\left(q_{\langle i}^{(\alpha)} - \frac{5}{2}\rho_\alpha \theta_\alpha u_{\langle i}^{(\alpha)}\right) \frac{\mathrm{D} v_{j\rangle}}{\mathrm{D} t} - \frac{14}{3}\sigma_{ij}^{(\alpha)} u_k^{(\alpha)} \frac{\mathrm{D} v_k}{\mathrm{D} t} \\
&\quad = \mathcal{P}_{ij}^{1(\alpha)} - 7\theta_\alpha \mathcal{P}_{ij}^{0(\alpha)} - \frac{7}{3}\sigma_{ij}^{(\alpha)} \frac{1}{\rho_\alpha}\mathcal{P}^{1(\alpha)} + 7\frac{1}{\rho_\alpha}\theta_\alpha \sigma_{ij}^{(\alpha)} \mathcal{P}^{0(\alpha)},
\end{aligned} \tag{7}$$

$$\begin{aligned}
&\frac{\partial \Delta_\alpha}{\partial t} + \frac{\partial(\Delta_\alpha v_i)}{\partial x_i} + \frac{4}{3}\Delta_\alpha \frac{\partial v_i}{\partial x_i} + 8\theta_\alpha \sigma_{ij}^{(\alpha)} \frac{\partial v_i}{\partial x_j} + 8\theta_\alpha \frac{\partial q_i^{(\alpha)}}{\partial x_i} + 28 q_i^{(\alpha)} \frac{\partial \theta_\alpha}{\partial x_i} - 20\rho_\alpha \theta_\alpha^2 \frac{\partial u_i^{(\alpha)}}{\partial x_i} \\
&\quad - 20\theta_\alpha^2 u_i^{(\alpha)} \frac{\partial \rho_\alpha}{\partial x_i} - 70\rho_\alpha \theta_\alpha u_i^{(\alpha)} \frac{\partial \theta_\alpha}{\partial x_i} + 4 R_{ij}^{(\alpha)} \frac{\partial v_i}{\partial x_j} + 8\left(q_i^{(\alpha)} - \frac{5}{2}\rho_\alpha \theta_\alpha u_i^{(\alpha)}\right) \frac{\mathrm{D} v_i}{\mathrm{D} t} = \mathcal{P}^{2(\alpha)} - 10\,\theta_\alpha \mathcal{P}^{1(\alpha)}.
\end{aligned} \tag{8}$$

Note that the contribution from the other component β in eqs. (1)–(8) appear only on the right-hand sides of these equations due to collisions of molecules of the gas α with molecules of the gas β. Furthermore, for $\gamma \in \{\alpha, \beta\}$, the quantities ρ_γ, $u_i^{(\gamma)}$, θ_γ, $\sigma_{ij}^{(\gamma)}$ and $q_i^{(\gamma)}$ in eqs. (1)–(8) are the density, diffusion velocity, temperature (in energy units), stress and heat flux, respectively, of the γ-species in the mixture; $m_{ijk}^{(\gamma)}$ is third degree moment; $R_{ij}^{(\gamma)}$ and Δ_γ are, respectively, related to the one-trace and full trace of the fourth moment and are defined in such a way that they vanish in 2×G13 theory (see [23]); and the Einstein summation applies over the repeated indices i, j, k, l, etc. The additional unknown v_i is the hydrodynamic velocity of the mixture obeying the total momentum balance equation

$$\rho\frac{\partial v_i}{\partial t} + \rho v_j\frac{\partial v_i}{\partial x_j} + \frac{\partial}{\partial x_j}\left(\sigma_{ij}^{(\alpha)} + \sigma_{ij}^{(\beta)}\right) + \frac{\partial}{\partial x_i}\left(\rho_\alpha\theta_\alpha + \rho_\beta\theta_\beta\right) = 0. \tag{9}$$

In the moment equations (1)–(8), the production terms $\mathcal{P}^{a(\alpha)}_{i_1 i_2 \dots i_n}$ for MM (denoted with subscripts '|MM') and HS (denoted with subscripts '|HS') on ignoring the nonlinear terms and using the abbreviation $\theta = (\theta_\alpha + \theta_\beta)/2$ read [23]

$$\mathcal{P}^{0(\alpha)}_{i|\mathrm{MM}} = -\frac{4}{3}a_1\nu_{\alpha\beta}\mu_\beta\rho_\alpha\left(u_i^{(\alpha)} - u_i^{(\beta)}\right), \tag{10}$$

$$\mathcal{P}^{1(\alpha)}_{|\mathrm{MM}} = -8a_1\mu_\alpha\mu_\beta k n_\alpha(T_\alpha - T_\beta), \tag{11}$$

$$\mathcal{P}^{0(\alpha)}_{ij|\mathrm{MM}} = -\nu_{\alpha\alpha}\sigma_{ij}^{(\alpha)} - 2\nu_{\alpha\beta}\mu_\beta\left[\sigma_{ij}^{(\alpha)} + \frac{1}{3}(4a_1-3)(\mu_\alpha-\mu_\beta)\sigma_{ij}^{(\alpha)} + \frac{1}{3}(4a_1-3)\mu_\beta\left(\sigma_{ij}^{(\alpha)} - \frac{\rho_\alpha}{\rho_\beta}\sigma_{ij}^{(\beta)}\right)\right], \tag{12}$$

$$\begin{aligned}\mathcal{P}^{1(\alpha)}_{i|\mathrm{MM}} = {}& -\frac{4}{3}\nu_{\alpha\alpha}h_i^{(\alpha)} - \frac{4}{3}\nu_{\alpha\beta}\mu_\beta\Big[2h_i^{(\alpha)} + 2(3a_1-1)(\mu_\alpha-\mu_\beta)h_i^{(\alpha)} + 10a_1\mu_\beta\theta\rho_\alpha\left(u_i^{(\alpha)} - u_i^{(\beta)}\right) \\ &+ 4(2a_1-1)\mu_\beta^2\left(h_i^{(\alpha)} - \frac{\rho_\alpha}{\rho_\beta}h_i^{(\beta)}\right)\Big],\end{aligned} \tag{13}$$

$$\mathcal{P}^{0(\alpha)}_{ijk|\mathrm{MM}} = -\frac{3}{2}\nu_{\alpha\alpha}m_{ijk}^{(\alpha)} - \nu_{\alpha\beta}\mu_\beta\left[3m_{ijk}^{(\alpha)} + (4a_1-3)(\mu_\alpha-\mu_\beta)m_{ijk}^{(\alpha)} + \frac{2}{3}(5a_3+3a_1-9)\mu_\beta^2\left(m_{ijk}^{(\alpha)} - \frac{\rho_\alpha}{\rho_\beta}m_{ijk}^{(\beta)}\right)\right], \tag{14}$$

$$\begin{aligned}\mathcal{P}^{1(\alpha)}_{ij|\mathrm{MM}} = {}& -\nu_{\alpha\alpha}\left(\frac{7}{6}R_{ij}^{(\alpha)} + 7\theta\sigma_{ij}^{(\alpha)}\right) - \nu_{\alpha\beta}\mu_\beta\Big[\frac{7}{3}R_{ij}^{(\alpha)} + 14\theta\sigma_{ij}^{(\alpha)} - \frac{14}{3}(\mu_\alpha-\mu_\beta)\big(3 - 2(4a_1-3)\mu_\beta\big)\theta\sigma_{ij}^{(\alpha)} \\ &+ \frac{1}{3}(\mu_\alpha-\mu_\beta)\Big\{(16a_1-7)\mu_\alpha^2 + (16a_1-6)\mu_\alpha\mu_\beta + (12a_3+20a_1-27)\mu_\beta^2\Big\}R_{ij}^{(\alpha)} \\ &+ \frac{28}{3}(4a_1-3)\mu_\beta^2\theta\left(\sigma_{ij}^{(\alpha)} - \frac{\rho_\alpha}{\rho_\beta}\sigma_{ij}^{(\beta)}\right) + \frac{4}{3}(3a_3+5a_1-7)\mu_\beta^3\left(R_{ij}^{(\alpha)} - \frac{\rho_\alpha}{\rho_\beta}R_{ij}^{(\beta)}\right)\Big],\end{aligned} \tag{15}$$

$$\begin{aligned}\mathcal{P}^{2(\alpha)}_{|\mathrm{MM}} = {}& -\frac{2}{3}\nu_{\alpha\alpha}\Delta_\alpha - \frac{4}{3}\nu_{\alpha\beta}\mu_\beta\Big[\Delta_\alpha + (\mu_\alpha-\mu_\beta)\Big\{(4a_1-1)\mu_\alpha^2 + 4a_1\mu_\alpha\mu_\beta + (8a_1-3)\mu_\beta^2\Big\}\Delta_\alpha \\ &+ 4(2a_1-1)\mu_\beta^3\left(\Delta_\alpha - \frac{\rho_\alpha}{\rho_\beta}\Delta_\beta\right) + 120a_1\mu_\beta\rho_\alpha\theta\frac{k(T_\alpha-T_\beta)}{m_\alpha+m_\beta}\Big],\end{aligned} \tag{16}$$

$$\mathcal{P}^{0(\alpha)}_{i|\mathrm{HS}} = -\nu_{\alpha\beta}\mu_\beta\left[\frac{5}{3}\rho_\alpha\left(u_i^{(\alpha)} - u_i^{(\beta)}\right) + \frac{1}{6\theta}\left(h_i^{(\alpha)} - \frac{\rho_\alpha}{\rho_\beta}h_i^{(\beta)}\right)\right], \tag{17}$$

$$\mathcal{P}^{1(\alpha)}_{|\mathrm{HS}} = -2\nu_{\alpha\beta}\mu_\beta\left[5\rho_\alpha\frac{k(T_\alpha-T_\beta)}{m_\alpha+m_\beta} + \frac{1}{12}\frac{1}{\theta}(\mu_\alpha-\mu_\beta)\Delta_\alpha + \frac{1}{12}\frac{1}{\theta}\mu_\beta\left(\Delta_\alpha - \frac{\rho_\alpha}{\rho_\beta}\Delta_\beta\right)\right] \tag{18}$$

$$\begin{aligned}\mathcal{P}^{0(\alpha)}_{ij|\mathrm{HS}} = {}& -\nu_{\alpha\alpha}\left(\sigma_{ij}^{(\alpha)} + \frac{1}{28\theta}R_{ij}^{(\alpha)}\right) - \nu_{\alpha\beta}\mu_\beta\Big[4\mu_\beta\left\{\sigma_{ij}^{(\alpha)} + \frac{1}{28\theta}R_{ij}^{(\alpha)} + \frac{1}{3}\left(\sigma_{ij}^{(\alpha)} - \frac{\rho_\alpha}{\rho_\beta}\sigma_{ij}^{(\beta)}\right) + \frac{1}{42\theta}\left(R_{ij}^{(\alpha)} - \frac{\rho_\alpha}{\rho_\beta}R_{ij}^{(\beta)}\right)\right\} \\ &+ \frac{1}{6}(\mu_\alpha-\mu_\beta)\left(20\sigma_{ij}^{(\alpha)} + \frac{1}{\theta}R_{ij}^{(\alpha)}\right)\Big],\end{aligned} \tag{19}$$

$$\begin{aligned}\mathcal{P}^{1(\alpha)}_{i|\mathrm{HS}} = {}& -\frac{4}{3}\nu_{\alpha\alpha}h_i^{(\alpha)} - 2\nu_{\alpha\beta}\mu_\beta\Big[\frac{8}{3}\mu_\beta h_i^{(\alpha)} + 5(\mu_\alpha-\mu_\beta)h_i^{(\alpha)} + \frac{1}{6}\mu_\beta(5+27\mu_\beta)\left(h_i^{(\alpha)} - \frac{\rho_\alpha}{\rho_\beta}h_i^{(\beta)}\right) \\ &+ \frac{5}{3}\mu_\beta(5+\mu_\beta)\rho_\alpha\theta\left(u_i^{(\alpha)} - u_i^{(\beta)}\right)\Big],\end{aligned} \tag{20}$$

$$\mathcal{P}^{0(\alpha)}_{ijk|\mathrm{HS}} = -\frac{3}{2}\nu_{\alpha\alpha}m^{(\alpha)}_{ijk} - \nu_{\alpha\beta}\mu_\beta\left[12\mu_\beta^2\left\{m^{(\alpha)}_{ijk} + \frac{3}{28}\left(m^{(\alpha)}_{ijk} - \frac{\rho_\alpha}{\rho_\beta}m^{(\beta)}_{ijk}\right)\right\} + (\mu_\alpha - \mu_\beta)(5+6\mu_\beta)m^{(\alpha)}_{ijk}\right], \tag{21}$$

$$\begin{aligned}\mathcal{P}^{1(\alpha)}_{ij|\mathrm{HS}} = &-\nu_{\alpha\alpha}\left(\frac{247}{168}R^{(\alpha)}_{ij} + \frac{15}{2}\theta\sigma^{(\alpha)}_{ij}\right)\\ &- \frac{1}{3}\nu_{\alpha\beta}\mu_\beta\Bigg[\frac{2}{7}\mu_\beta^3\left\{247R^{(\alpha)}_{ij} + 1260\theta\sigma^{(\alpha)}_{ij} + 88\left(R^{(\alpha)}_{ij} - \frac{\rho_\alpha}{\rho_\beta}R^{(\beta)}_{ij}\right) + 448\theta\left(\sigma^{(\alpha)}_{ij} - \frac{\rho_\alpha}{\rho_\beta}\sigma^{(\beta)}_{ij}\right)\right\}\\ &+ (\mu_\alpha - \mu_\beta)\left(\frac{1}{7}(140 + 63\mu_\beta + 395\mu_\beta^2)R^{(\alpha)}_{ij} - 4\mu_\beta^2\frac{\rho_\alpha}{\rho_\beta}R^{(\beta)}_{ij} + 28\mu_\beta(5+9\mu_\beta)\theta\sigma^{(\alpha)}_{ij} - 56\mu_\beta^2\frac{\rho_\alpha}{\rho_\beta}\theta\sigma^{(\beta)}_{ij}\right)\Bigg],\end{aligned} \tag{22}$$

$$\begin{aligned}\mathcal{P}^{2(\alpha)}_{|\mathrm{HS}} = &-\frac{2}{3}\nu_{\alpha\alpha}\Delta_\alpha - \nu_{\alpha\beta}\mu_\beta\Bigg[\frac{32}{3}\mu_\beta^3\Delta_\alpha + \frac{2}{3}(\mu_\alpha - \mu_\beta)(10 + 3\mu_\beta + 23\mu_\beta^2)\Delta_\alpha\\ &+ \frac{10}{3}\mu_\beta^2(1+3\mu_\beta)\left(\Delta_\alpha - \frac{\rho_\alpha}{\rho_\beta}\Delta_\beta\right) + 40\mu_\beta(5+\mu_\beta)\rho_\alpha\theta\frac{k(T_\alpha - T_\beta)}{m_\alpha + m_\beta}\Bigg].\end{aligned} \tag{23}$$

In the production terms above,

$$\mu_\alpha = \frac{m_\alpha}{m_\alpha + m_\beta} \quad \text{and} \quad \mu_\beta = \frac{m_\beta}{m_\alpha + m_\beta} \tag{24}$$

are the mass ratios of the α- and β-constituents, respectively, with m_α and m_β being the masses of the α- and β-constituents, and the collision frequencies $\nu_{\alpha\alpha}$ and $\nu_{\alpha\beta}$ are defined as

$$\nu_{ij} = \frac{16}{5}\sqrt{\pi}\, n_j\, \Omega^{(2,2)}_{ij}\sqrt{\frac{\theta_i + \theta_j}{2}}, \quad i, j \in \{\alpha, \beta\} \tag{25}$$

where $\Omega^{(l,r)}_{ij}$ for $i, j \in \{\alpha, \beta\}$ are the standard Omega integrals [5, 23]. The constants a_r's appearing in the production terms for MM are defined as $a_r = A_r/A_2$ [5] with

$$A_r = \sqrt{2}\int_0^{\pi/4}\frac{1 - (-1)^r\cos^r(2\zeta)}{\sin^2(2\phi)}\,\mathrm{d}\phi\,; \qquad \zeta = \sqrt{\cos(2\phi)}\int_0^{\pi/2}\frac{\mathrm{d}\psi}{\sqrt{1 - \sin^2\phi\,\sin^2\psi}}. \tag{26}$$

The numerical values of the first few constants are $a_1 = 0.9673 \approx 29/30$, $a_2 = 1$, $a_3 = 1.3416 \approx 51/38$.

The G26 equations for the β-component in the mixture can be written analogously by interchanging α and β in eqs. (1)–(8) and in the production terms (10)–(23). The G26 equations for both the species along with the total momentum balance equation (9) constitute the 2×G26 equations for a binary mixture of gases α and β. It should be noted that the total momentum balance equation (9) is required as v_i appears as an additional variable in the 2×G26 equation. Nonetheless, the diffusion velocities in a binary gas mixture are not independent and are related via $\rho_\alpha u^{(\alpha)}_i + \rho_\beta u^{(\beta)}_i = 0$. Consequently, the balance equation for the diffusion velocity of any one component (say, β) can be discarded while including the total momentum balance equation. Thus, the number of independent equations in the system remains equal to that in the 2×G26 system, and we still refer that system as the 2×G26 system. The system of 2×G13 equations can be obtained easily from the 2×G26 system by ignoring the balance equations for $m^{(\alpha)}_{ijk}$, $m^{(\beta)}_{ijk}$, $R^{(\alpha)}_{ij}$, $R^{(\beta)}_{ij}$, Δ_α and Δ_β and replacing these variables with zero in the other equations and corresponding production terms.

Boundary conditions

It is assumed that none of the gas molecules can penetrate through the walls; consequently, the normal components (denoted by subscripts "n") of the diffusion velocities of the gases in the mixture also vanish at the wall. This leads to boundary conditions

$$u^{(\gamma)}_n\Big|_{\mathrm{wall}} = 0 \quad \text{for} \quad \gamma \in \{\alpha, \beta\}. \tag{27}$$

Typically, additional conditions on the mass conservation of individual constituents are also required which state that the mass of the each constituent γ ($\gamma \in \{\alpha,\beta\}$) in a given domain Γ must be equal to a given value $M_0^{(\gamma)}$, i.e.,

$$\int_\Gamma \rho_\gamma \,\mathrm{d}V = M_0^{(\gamma)}, \tag{28}$$

where $\mathrm{d}V$ is infinitesimal control volume in the domain Γ. The other boundary conditions are derived using the Maxwell accommodation model [47]. For conciseness, the detailed derivation of the other boundary conditions is not presented here but can be found in [23]. Ultimately, the remaining boundary conditions for the 2×G13 equations turn out to be ($\gamma \in \{\alpha,\beta\}$) [23]

$$\sigma_{nt_i}^{(\gamma)} = -\frac{\chi_\gamma}{2-\chi_\gamma}\sqrt{\frac{2}{\pi\theta_\gamma}}\left[P_\gamma V_{t_i} + \frac{1}{2}\rho_\gamma\theta_\gamma u_{t_i}^{(\gamma)} + \frac{1}{5}q_{t_i}^{(\gamma)}\right], \tag{29}$$

$$q_n^{(\gamma)} = -\frac{\chi_\gamma}{2-\chi_\gamma}\sqrt{\frac{2}{\pi\theta_\gamma}}\left[2P_\gamma(\theta_\gamma - \theta_w^{(\gamma)}) + \frac{1}{2}\theta_\gamma\sigma_{nn}^{(\gamma)} - \frac{1}{2}P_\gamma V^2\right], \tag{30}$$

where n and t_i denote the normal and tangential components, respectively; $0 \le \chi_\gamma \le 1$ is the accommodation coefficient—used as a parameter for gas-wall interaction in the Maxwell accommodation model [47]—for the γ-constituent in the mixture; V_{t_i} is the tangential component of the slip velocity $\boldsymbol{V} = \boldsymbol{v} - \boldsymbol{v}_w$ with $\boldsymbol{v}_w$ being the velocity of the wall; $\theta_w^{(\gamma)} = kT_w/m_\gamma$ with k and T_w being the Boltzmann constant and the temperature of the wall, respectively; and $P_\gamma = \rho_\gamma\theta_\gamma + \frac{1}{2}\sigma_{nn}^{(\gamma)}$.

The remaining boundary conditions for the 2×G26 equations turn out to be ($\gamma \in \{\alpha,\beta\}$) [22, 23]

$$\sigma_{nt_i}^{(\gamma)} = -\frac{\chi_\gamma}{2-\chi_\gamma}\sqrt{\frac{2}{\pi\theta_\gamma}}\left[P_\gamma V_{t_i} + \frac{1}{2}\rho_\gamma\theta_\gamma u_{t_i}^{(\gamma)} + \frac{1}{5}q_{t_i}^{(\gamma)} + \frac{1}{2}m_{nnt_i}^{(\gamma)}\right], \tag{31}$$

$$q_n^{(\gamma)} = -\frac{\chi_\gamma}{2-\chi_\gamma}\sqrt{\frac{2}{\pi\theta_\gamma}}\left[2P_\gamma(\theta_\gamma - \theta_w^{(\gamma)}) + \frac{1}{2}\theta_\gamma\sigma_{nn}^{(\gamma)} + \frac{5}{28}R_{nn}^{(\gamma)} + \frac{1}{15}\Delta_\gamma - \frac{1}{2}P_\gamma V^2\right], \tag{32}$$

$$m_{nnn}^{(\gamma)} = \frac{\chi_\gamma}{2-\chi_\gamma}\sqrt{\frac{2}{\pi\theta_\gamma}}\left[\frac{2}{5}P_\gamma(\theta_\gamma - \theta_w^{(\gamma)}) - \frac{7}{5}\theta_\gamma\sigma_{nn}^{(\gamma)} - \frac{1}{14}R_{nn}^{(\gamma)} + \frac{1}{75}\Delta_\gamma - \frac{3}{5}P_\gamma V^2\right], \tag{33}$$

$$m_{nt_it_i}^{(\gamma)} = -\frac{\chi_\gamma}{2-\chi_\gamma}\sqrt{\frac{2}{\pi\theta_\gamma}}\left[\frac{1}{5}P_\gamma(\theta_\gamma - \theta_w^{(\gamma)}) - \frac{1}{5}\theta_\gamma\sigma_{nn}^{(\gamma)} + \theta_\gamma\sigma_{t_it_i}^{(\gamma)} + \frac{1}{14}R_{t_it_i}^{(\gamma)} + \frac{1}{150}\Delta_\gamma + \frac{1}{5}P_\gamma V^2 - P_\gamma V_{t_i}^2\right], \tag{34}$$

$$m_{nt_1t_2}^{(\gamma)} = -\frac{\chi_\gamma}{2-\chi_\gamma}\sqrt{\frac{2}{\pi\theta_\gamma}}\left[\theta_\gamma\sigma_{t_1t_2}^{(\gamma)} + \frac{1}{14}R_{t_1t_2}^{(\gamma)} - P_\gamma V_{t_1}V_{t_2}\right], \tag{35}$$

$$R_{nt_i}^{(\gamma)} = \frac{\chi_\gamma}{2-\chi_\gamma}\sqrt{\frac{2}{\pi\theta_\gamma}}\left[6P_\gamma(\theta_\gamma - \theta_w^{(\gamma)})V_{t_i} + P_\gamma\theta_\gamma V_{t_i} + \frac{13}{2}\rho_\gamma\theta_\gamma^2 u_{t_i}^{(\gamma)} - \frac{11}{5}\theta_\gamma q_{t_i}^{(\gamma)} - \frac{1}{2}\theta_\gamma m_{nnt_i}^{(\gamma)} - P_\gamma V^2 V_{t_i}\right], \tag{36}$$

where $P_\gamma = \rho_\gamma\theta_\gamma + \frac{1}{2}\sigma_{nn}^{(\gamma)} - \frac{1}{28}\frac{R_{nn}^{(\gamma)}}{\theta_\gamma} - \frac{1}{120}\frac{\Delta_\gamma}{\theta_\gamma}$.

Linear-dimensionless moment equations in one-dimension

The equations and boundary conditions presented in the previous section are linearized around a reference state given by constant number densities of individual components n_α^0, n_β^0, a constant common temperature of the mixture T_0 and the other field variables being zero, i.e.,

$$\left.\begin{aligned} &v_i = \varepsilon\,\tilde{v}_i, \quad n_\gamma = n_\gamma^0 + \varepsilon\,\tilde{n}_\gamma, \quad T_\gamma = T_0 + \varepsilon\,\tilde{T}_\gamma, \quad u_i^{(\gamma)} = \varepsilon\,\tilde{u}_i^{(\gamma)}, \quad \sigma_{ij}^{(\gamma)} = \varepsilon\,\tilde{\sigma}_{ij}^{(\gamma)}, \\ &q_i^{(\gamma)} = \varepsilon\,\tilde{q}_i^{(\gamma)}, \quad m_{ijk}^{(\gamma)} = \varepsilon\,\tilde{m}_{ijk}^{(\gamma)}, \quad R_{ij}^{(\gamma)} = \varepsilon\,\tilde{R}_{ij}^{(\gamma)}, \quad \Delta_\gamma = \varepsilon\,\tilde{\Delta}_\gamma, \quad \text{for} \quad \gamma \in \{\alpha,\beta\}, \end{aligned}\right\} \tag{37}$$

where $\gamma \in \{\alpha,\beta\}$, $n_\gamma = \rho_\gamma/m_\gamma$ is the number density of the γ-constituent, and tilde denotes the perturbed variables. Note that the small parameter for linearization is ε, the one used to depict the different temperatures on the plates in the problem. Furthermore, the resulting linearized equations are made dimensionless using the length scale as L (the gap between plates), velocity scale as $v_0 = \sqrt{kT_0/m}$ and time scale as L/v_0, where $m = \mathrm{x}_\alpha^0 m_\alpha + \mathrm{x}_\beta^0 m_\beta$ is the mean molecular mass of the mixture with $\mathrm{x}_\gamma^0 = n_\gamma^0/(n_\alpha^0 + n_\beta^0)$ being the mole fraction of the γ-constituent ($\gamma \in \{\alpha,\beta\}$) in the reference state; and the other field variables are scaled with the appropriate combinations of n_α^0, n_β^0 and T_0. The dimensionless variables (denoted with hats) read ($\gamma \in \{\alpha,\beta\}$)

$$\left.\begin{aligned} &\hat{v}_i = \frac{\tilde{v}_i}{v_0}, \quad \hat{n}_\gamma = \frac{\tilde{n}_\gamma}{n_\gamma^0}, \quad \hat{T}_\gamma = \frac{\tilde{T}_\gamma}{T_0}, \quad \hat{u}_i^{(\gamma)} = \frac{\tilde{u}_i^{(\gamma)}}{(\theta_\gamma^0)^{1/2}}, \quad \hat{\sigma}_{ij}^{(\gamma)} = \frac{\tilde{\sigma}_{ij}^{(\gamma)}}{\rho_\gamma^0\theta_\gamma^0}, \\ &\hat{q}_i^{(\gamma)} = \frac{\tilde{q}_i^{(\gamma)}}{\rho_\gamma^0(\theta_\gamma^0)^{3/2}}, \quad \hat{m}_{ijk}^{(\gamma)} = \frac{\tilde{m}_{ijk}^{(\gamma)}}{\rho_\gamma^0(\theta_\gamma^0)^{3/2}}, \quad \hat{R}_{ij}^{(\gamma)} = \frac{\tilde{R}_{ij}^{(\gamma)}}{\rho_\gamma^0(\theta_\gamma^0)^{2}}, \quad \hat{\Delta}_\gamma = \frac{\tilde{\Delta}_\gamma}{\rho_\gamma^0(\theta_\gamma^0)^{2}}, \end{aligned}\right\} \tag{38}$$

where $\rho_\gamma^0 = m_\gamma n_\gamma^0$, $\theta_\gamma^0 = kT_0/m_\gamma$ and the quantities with hats denote the dimensionless perturbations in field variables from their respective reference states.

For the problem under consideration, heat transfer takes place only in the x-direction. Therefore, it is convenient to write all the equations in one dimension (1D). The linear-dimensionless G26 equations for the α-constituent in a binary gas mixture comprising of the α and β gases in steady state ($\partial(\cdot)/\partial t = 0$) at rest ($v_x = 0$) read [23]

$$\frac{\partial \hat{u}_x^{(\alpha)}}{\partial \hat{x}} = 0, \tag{39}$$

$$\frac{\partial \hat{\sigma}_{xx}^{(\alpha)}}{\partial \hat{x}} + \frac{\partial \hat{T}_\alpha}{\partial \hat{x}} + \frac{\partial \hat{n}_\alpha}{\partial \hat{x}} = -\frac{1}{\mathrm{Kn}\,\Omega}\mathrm{x}_\beta^0\left(\delta_1\hat{u}_x^{(\alpha)} + \delta_2\hat{q}_x^{(\alpha)} - \delta_3\hat{u}_x^{(\beta)} - \delta_4\hat{q}_x^{(\beta)}\right), \tag{40}$$

$$-\frac{3}{2}\frac{\partial \hat{u}_x^{(\alpha)}}{\partial \hat{x}} + \frac{\partial \hat{q}_x^{(\alpha)}}{\partial \hat{x}} = -\frac{1}{\mathrm{Kn}\,\Omega}\mathrm{x}_\beta^0\left[\delta_5(\hat{T}_\alpha - \hat{T}_\beta) + \delta_6\hat{\Delta}_\alpha - \delta_7\hat{\Delta}_\beta\right], \tag{41}$$

$$\frac{\partial \hat{m}_{xxx}^{(\alpha)}}{\partial \hat{x}} + \frac{8}{15}\frac{\partial \hat{q}_x^{(\alpha)}}{\partial \hat{x}} = -\frac{1}{\mathrm{Kn}\,\Omega}\left[\mathrm{x}_\alpha^0\Omega_\alpha\left(\hat{\sigma}_{xx}^{(\alpha)} + \delta_8\hat{R}_{xx}^{(\alpha)}\right) + \mathrm{x}_\beta^0\left(\delta_9\hat{\sigma}_{xx}^{(\alpha)} + \delta_{10}\hat{R}_{xx}^{(\alpha)} - \delta_{11}\hat{\sigma}_{xx}^{(\beta)} - \delta_{12}\hat{R}_{xx}^{(\beta)}\right)\right], \tag{42}$$

$$\begin{aligned} &\frac{1}{2}\frac{\partial \hat{R}_{xx}^{(\alpha)}}{\partial \hat{x}} + \frac{7}{2}\frac{\partial \hat{\sigma}_{xx}^{(\alpha)}}{\partial \hat{x}} + \frac{1}{6}\frac{\partial \hat{\Delta}_\alpha}{\partial \hat{x}} + 5\frac{\partial \hat{T}_\alpha}{\partial \hat{x}} + \frac{5}{2}\frac{\partial \hat{n}_\alpha}{\partial \hat{x}} \\ &\quad = -\frac{1}{\mathrm{Kn}\,\Omega}\left[\frac{2}{3}\mathrm{x}_\alpha^0\Omega_\alpha\left(\hat{q}_x^{(\alpha)} - \frac{5}{2}\hat{u}_x^{(\alpha)}\right) + \mathrm{x}_\beta^0\left(\delta_{13}\hat{q}_x^{(\alpha)} - \delta_{14}\hat{u}_x^{(\alpha)} - \delta_{15}\hat{q}_x^{(\beta)} - \delta_{16}\hat{u}_x^{(\beta)}\right)\right], \end{aligned} \tag{43}$$

$$\frac{9}{35}\frac{\partial \hat{R}_{xx}^{(\alpha)}}{\partial \hat{x}} + \frac{9}{5}\frac{\partial \hat{\sigma}_{xx}^{(\alpha)}}{\partial \hat{x}} = -\frac{1}{\mathrm{Kn}\,\Omega}\left[\frac{3}{2}\mathrm{x}_\alpha^0\Omega_\alpha\hat{m}_{xxx}^{(\alpha)} + \mathrm{x}_\beta^0\left(\delta_{17}\hat{m}_{xxx}^{(\alpha)} - \delta_{18}\hat{m}_{xxx}^{(\beta)}\right)\right], \tag{44}$$

$$2\frac{\partial \hat{m}_{xxx}^{(\alpha)}}{\partial \hat{x}} + \frac{56}{15}\frac{\partial \hat{q}_x^{(\alpha)}}{\partial \hat{x}} - \frac{28}{3}\frac{\partial \hat{u}_x^{(\alpha)}}{\partial \hat{x}} = -\frac{1}{\mathrm{Kn}\,\Omega}\left[\mathrm{x}_\alpha^0\Omega_\alpha\left(\delta_{19}\hat{R}_{xx}^{(\alpha)} + \delta_{20}\hat{\sigma}_{xx}^{(\alpha)}\right) + \mathrm{x}_\beta^0\left(\delta_{21}\hat{R}_{xx}^{(\alpha)} + \delta_{22}\hat{\sigma}_{xx}^{(\alpha)} - \delta_{23}\hat{R}_{xx}^{(\beta)} - \delta_{24}\hat{\sigma}_{xx}^{(\beta)}\right)\right], \tag{45}$$

$$8\frac{\partial \hat{q}_x^{(\alpha)}}{\partial \hat{x}} - 20\frac{\partial \hat{u}_x^{(\alpha)}}{\partial \hat{x}} = -\frac{1}{\mathrm{Kn}\,\Omega}\left[\frac{2}{3}\mathrm{x}_\alpha^0\Omega_\alpha\hat{\Delta}_\alpha + \mathrm{x}_\beta^0\left\{\delta_{25}\hat{\Delta}_\alpha - \delta_{26}\hat{\Delta}_\beta + \delta_{27}(\hat{T}_\alpha - \hat{T}_\beta)\right\}\right], \tag{46}$$

where

$$\mathrm{Kn} = \frac{\ell}{L} \quad \text{with} \quad \ell = \frac{5}{16\sqrt{\pi}\,n_0\left(\mathrm{x}_\alpha^0\Omega_{\alpha\alpha}^{(2,2)} + \mathrm{x}_\beta^0\Omega_{\beta\beta}^{(2,2)}\right)} \tag{47}$$

is the Knudsen number;

$$\Omega_\alpha = \frac{\Omega_{\alpha\alpha}^{(2,2)}}{\Omega_{\alpha\beta}^{(2,2)}} \qquad \text{and} \qquad \Omega_\beta = \frac{\Omega_{\beta\beta}^{(2,2)}}{\Omega_{\alpha\beta}^{(2,2)}} \tag{48}$$

are the ratios directly related to the collisional cross sections; $\Omega = \mathrm{x}_\alpha^0\Omega_\alpha + \mathrm{x}_\beta^0\Omega_\beta$; and the coefficients δ_8, δ_{19}, δ_{20} are constants while the other δ_i's depend only on the mass ratios of the constituents given by (24). The explicit values of δ_i's are not given here for brevity but for MM and HS, they can be found in [23]. All the quantities in (39)–(46) and henceforth are dimensionless.

The one-dimensional G26 equations for the β-constituent follow by interchanging α and β in (39)–(46), and the total momentum balance equation (9) in the dimensionless steady-state form and in 1D reads

$$\mathrm{x}_\alpha^0\left(\frac{\partial\hat{\sigma}_{xx}^{(\alpha)}}{\partial\hat{x}}+\frac{\partial\hat{n}_\alpha}{\partial\hat{x}}+\frac{\partial\hat{T}_\alpha}{\partial\hat{x}}\right)+\mathrm{x}_\beta^0\left(\frac{\partial\hat{\sigma}_{xx}^{(\beta)}}{\partial\hat{x}}+\frac{\partial\hat{n}_\beta}{\partial\hat{x}}+\frac{\partial\hat{T}_\beta}{\partial\hat{x}}\right)=0. \tag{49}$$

Therefore, the system of linear-dimensionless 2×G26 equations for the problem under consideration consists of equations (39)–(46), similar equations for the β-constituent and equation (49), where the balance equation for the diffusion velocity of the β-constituent is discarded, and the diffusion velocity of the β-constituent in other equations is eliminated in terms of the diffusion velocity of the α-constituent.

Analogously, the system of linear-dimensionless 2×G13 equations for the problem under consideration consists of equations (39)–(43) with $\hat{m}_{xxx}^{(\alpha)} = \hat{m}_{xxx}^{(\beta)} = \hat{R}_{xx}^{(\alpha)} = \hat{R}_{xx}^{(\beta)} = \hat{\Delta}_\alpha = \hat{\Delta}_\beta = 0$, similar equations for the β-constituent and equation (49), where the balance equation for the diffusion velocity of the β-constituent is discarded, and the diffusion velocity of the β-constituent in the other equations is eliminated in terms of the diffusion velocity of the α-constituent.

Linear-dimensionless boundary conditions

For the above one-dimensional problem, the relevant boundary conditions associated with the 2×G13 equations are conditions (27)–(30) for each constituent while those associated with the 2×G26 equations are conditions (27), (28) and (31)–(33) for each constituent. Note that boundary conditions (29) and (31) for the problem under consideration just imply that the slip velocity vanishes, i.e, $\boldsymbol{V} = \boldsymbol{0}$, and the other boundary conditions—for the problem under consideration—in linear-dimensionless form are as follows. Boundary conditions (27) and (28) read

$$\hat{u}_x^{(\gamma)}\left(-\frac{1}{2}\right)=\hat{u}_x^{(\gamma)}\left(\frac{1}{2}\right)=0 \quad \text{for} \quad \gamma\in\{\alpha,\beta\}. \tag{50}$$

$$\int_{-1/2}^{1/2}\hat{n}_\gamma\,\mathrm{d}\hat{x}=0 \quad \text{for} \quad \gamma\in\{\alpha,\beta\}. \tag{51}$$

The remaining boundary conditions associated with 2×G13 equations, (30), read ($\gamma \in \{\alpha,\beta\}$)

$$\hat{q}_x^{(\gamma)}=-\mathrm{n}_x\frac{\chi_\gamma}{2-\chi_\gamma}\sqrt{\frac{2}{\pi}}\left[2\left(\hat{T}_\gamma-\mathrm{n}_x\frac{\Delta\hat{T}_w}{2}\right)+\frac{1}{2}\hat{\sigma}_{xx}^{(\gamma)}\right], \tag{52}$$

while the remaining boundary conditions associated with 2×G26 equations, (32) and (33), read ($\gamma \in \{\alpha,\beta\}$)

$$\hat{q}_x^{(\gamma)}=-\mathrm{n}_x\frac{\chi_\gamma}{2-\chi_\gamma}\sqrt{\frac{2}{\pi}}\left[2\left(\hat{T}_\gamma-\mathrm{n}_x\frac{\Delta\hat{T}_w}{2}\right)+\frac{1}{2}\hat{\sigma}_{xx}^{(\gamma)}+\frac{5}{28}\hat{R}_{xx}^{(\gamma)}+\frac{1}{15}\hat{\Delta}_\gamma\right], \tag{53}$$

$$\hat{m}_{xxx}^{(\gamma)}=\mathrm{n}_x\frac{\chi_\gamma}{2-\chi_\gamma}\sqrt{\frac{2}{\pi}}\left[\frac{2}{5}\left(\hat{T}_\gamma-\mathrm{n}_x\frac{\Delta\hat{T}_w}{2}\right)-\frac{7}{5}\hat{\sigma}_{xx}^{(\gamma)}-\frac{1}{14}\hat{R}_{xx}^{(\gamma)}+\frac{1}{75}\hat{\Delta}_\gamma\right], \tag{54}$$

where $\mathrm{n}_x = 1$ for the left plate while $\mathrm{n}_x = -1$ for the right plate, and $\Delta\hat{T}_w = \Delta\tilde{T}_w/T_0$.

The above-mentioned systems of moment equations for the problem along with the above-mentioned boundary conditions have been solved numerically using the finite difference method, for which the (dimensionless) gap between the plates has been discretized into 101 equispaced points (or into 100 intervals of equal size). For discretization, the central difference scheme at interior points while the forward and backward difference schemes at left- and right-endpoints, respectively, have been employed. Further details on the numerical method are skipped here for the sake of brevity but they can be found in Section 7.1 of Reference [23]. The method gives solutions within a few seconds for both the interaction potentials.

RESULTS

Following [1], we shall compute the dimensionless total heat flux between the plates $\hat{q}_x$, given by,

$$\hat{q}_x = \frac{q_x}{\sqrt{2}\, n_0 k T_0 v_0 \Delta \hat{T}_w} = \sqrt{\frac{\mu_\alpha \mathrm{x}_\alpha^0 + \mu_\beta \mathrm{x}_\beta^0}{2}} \left(\frac{\mathrm{x}_\alpha^0}{\sqrt{\mu_\alpha}} \hat{q}_x^{(\alpha)} + \frac{\mathrm{x}_\beta^0}{\sqrt{\mu_\beta}} \hat{q}_x^{(\beta)} \right) \frac{1}{\Delta \hat{T}_w} \tag{55}$$

for three noble gas mixtures: neon–argon (Ne–Ar), helium–argon (He–Ar) and helium–xenon (He–Xe) through the 2×G13 and 2×G26 equations, both for MM and HS, and compare the results with those in [1]—obtained by solving the Boltzmann–McCormack kinetic equation by the discrete velocity method with an implementation of the so-called realistic interaction potential. The dimensionless heat flux is taken in the form of (55) in order to compare our results with those in [1]. The diffuse scattering boundary conditions considered in [1] correspond to the boundary conditions with accommodation coefficients $\chi_\alpha = \chi_\beta = 1$. It should also be noted that the rarefaction parameter $\delta = LkT_0 n_0/(\sqrt{2}\,\eta v_0)$ used in [1] relates to the Knudsen number $(47)_1$ by $\mathrm{Kn} = 1/(\sqrt{2}\,\delta)$, which leads to an expression for the viscosity of a binary gas mixture

$$\eta = \frac{5}{16\sqrt{\pi}} \frac{\sqrt{kT_0 m}}{\left(\mathrm{x}_\alpha^0 \Omega_{\alpha\alpha}^{(2,2)} + \mathrm{x}_\beta^0 \Omega_{\beta\beta}^{(2,2)}\right)}. \tag{56}$$

This expression gives reasonable agreement with viscosities of binary gas mixtures obtained through experimental data at 300 K given in [48]. Nevertheless, a viscosity formula for binary gas mixtures can also be obtained through a rigorous Chapman–Enskog expansion on the moment equations, see [24]. The mixtures considered are in order of small-to-large mass differences and the molecular masses of the gases constituting these mixtures are $m_{\mathrm{He}} = 4.0026$, $m_{\mathrm{Ne}} = 20.1791$, $m_{\mathrm{Ar}} = 39.948$, $m_{\mathrm{Xe}} = 131.293$ in atomic units. The ratios Ω_α and Ω_β for these mixtures are given in Table 1, see [23].

TABLE 1. Ratios Ω_α and Ω_β

Mixture	Ω_α	Ω_β
Ne–Ar	0.6907	1.3664
He–Ar	0.5631	1.5615
He–Xe	0.3843	1.9046

Figures 2 and 3 illustrate the variation of the total heat flux with change in mole fraction of the lighter gas in each mixture for Kn = 0.0707 ($\delta = 10$) and Kn = 0.7071 ($\delta = 1$), respectively. The small circles in Figures 2 and 3 denote the data from [1] obtained by solving the Boltzmann–McCormack kinetic equation by the discrete velocity method with an implementation of the realistic interaction potential. The red, blue and green colors (for small circles as well as for the lines) in each figure correspond to results for Ne–Ar, He–Ar and He–Xe mixtures, respectively. Moreover, in both Figures 2 and 3, the top and bottom rows exhibit the solutions for MM and HS, respectively, whereas the left and right columns display the solutions from 2×G13 equations and 2×G26 equations, respectively. From Figures 2 and 3, the following points are deduced.

1. The total heat flux of the mixture increases with increasing rarefaction. All types of Grad moment system under consideration for both MM and HS confirm this. A detailed quantitative comparison of the total heat fluxes, even for high Knudsen numbers, in case of 2×G26 equations with MM can be found in [22]. It should also be noticed that although both Grad moment systems (2×G13 as well as 2×G26) for MM overestimate the actual results in general, the results from them are not very far from those of [1].
2. In general, the results obtained through 2×G26 equations—in comparison with those obtained through 2×G13 equations—are closer to the results of [1].
3. In case of MM (top row in each figure), the results are closer to those from [1] when the mixture is less rarefied, i.e., for the smaller Knudsen number (Kn = 0.0707). This means that as rarefaction increases, the results starts deviating more from the actual ones. Consequently, it might be necessary to include more and more moments into the system with increasing rarefaction.

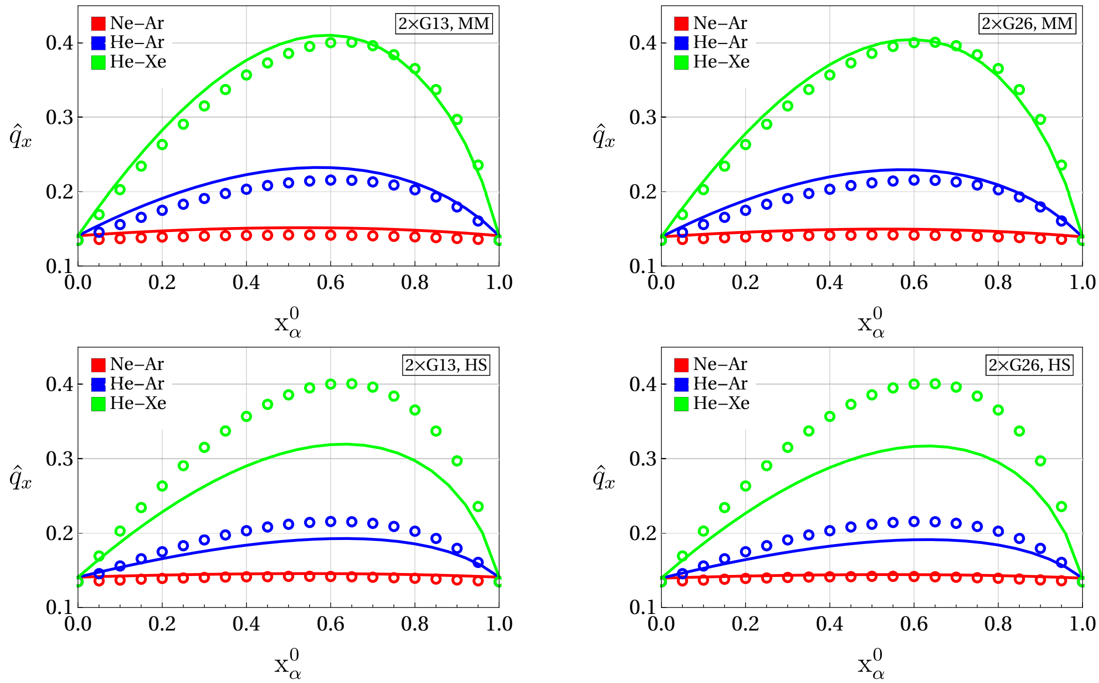

FIGURE 2. Dimensionless total heat flux $\hat{q}_x$ plotted over the mole fraction of the lighter gases x_α^0 in the mixtures of Ne–Ar, He–Ar and He–Xe for Kn = 0.0707. The circles denote the data from [1] obtained using realistic potential. The top and bottom rows of the figure depict the solutions for MM and HS, respectively, whereas the left and right columns show the solutions through 2×G13 equations and 2×G26 equations, respectively.

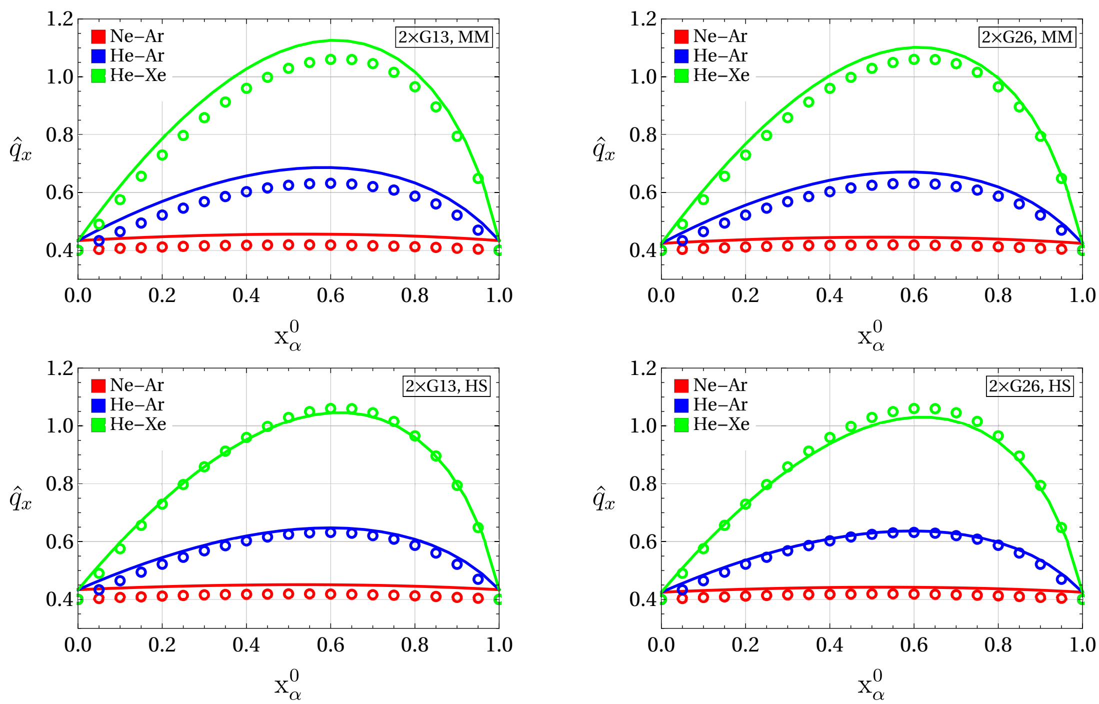

FIGURE 3. Same as Figure 2 but for Kn = 0.7071.

4. On the contrary, the results in case of HS (bottom row in each figure) match very well with those from [1] when the mixture is more rarefied (Figure 3) whereas when the mixture is less rarefied the results from the moment equations underestimate the actual results significantly, although the qualitative behaviour of the former remains very similar to the latter. It is also clear from the bottom row of Figure 2 that the most significant difference in results from moment equations and those from [1] is for He–Xe mixture, which is the case of large mass differences; for small mass difference (Ne–Ar), the two results match quite well when the rarefaction is small (Kn $= 0.0707$). In other words, for small rarefaction and HS (bottom row of Figure 2), the deviation in results from the moment equations and the actual results increases with increasing mass differences in the mixture. In fact, the authors of [1] have also pointed out that in the hydrodynamic/slip-flow regime, i.e., when Kn $\lesssim 0.0707$, the total heat flux computed with HS can deviate up to 15% from that computed with realistic potential whereas in the transition regime, i.e., when Kn $\gtrsim 0.7071$, the difference in heat flux computed with HS and that computed with realistic potential remains less than 5%.
5. Similar to [1], the results from all types of moment equations under consideration also confirm that the maximum heat flux is observed when the mole fraction of the lighter gas in the mixture is around 0.62.

CONCLUSION

We studied the problem of heat transfer in two-component gas mixtures of noble (monatomic) gases confined between two infinite parallel plates having different temperatures through the Grad moment equations for MM and HS. We found that the results from the moment systems under consideration agree with those from [1], at least qualitatively, including the results for HS at Kn $= 0.0707$ (bottom row of Figure 2). Still, possible reasons for the deviations in the results are the use of an interaction potentials based on MM and HS which influence the form of the productions terms in the moment system, and the use of a simplified expression for the mean free path $(47)_2$ implying the viscosity formula (56). It may also be inferred from Figures 2 and 3 as well as from the above discussion that as an alternative to the realistic potential, the Maxwell interaction potential could be a preferable choice over the hard-sphere interaction potential in the hydrodynamic/slip-flow regime while the hard-sphere interaction potential could be a preferable choice over the Maxwell interaction potential in the transition regime. Thus, the moment equations for gas mixtures provide an enticing and reliable framework as an alternative to the computationally expensive methods.

ACKNOWLEDGMENTS

VKG gratefully acknowledges the funding from the SERB India through "MATRICS" project MTR/2017/000693 and financial support through the Commonwealth Rutherford Fellowship.

REFERENCES

[1] F. Sharipov, L. M. G. Cumin, and D. Kalempa, Physica A **378**, 183–193 (2007).
[2] S. Chapman and T. G. Cowling, "The mathematical theory of non-uniform gases," (Cambridge University Press, Cambridge, 1970).
[3] C. Cercignani, "Rarefied gas dynamics: From basic concepts to actual calculations," (Cambridge University Press, Cambridge, 2000).
[4] H. Struchtrup, "Macroscopic transport equations for rarefied gas flows," (Springer, Berlin, 2005).
[5] G. M. Kremer, "An introduction to the Boltzmann equation and transport processes in gases," (Springer, Berlin, 2010).
[6] M. Torrilhon, Annu. Rev. Fluid Mech. **48**, 429–458 (2016).
[7] A. S. Rana, V. K. Gupta, and H. Struchtrup, Proc. Roy. Soc. A **474**, p. 20180323 (2018).
[8] H. Grad, Comm. Pure Appl. Math. **2**, 331–407 (1949).
[9] H. Struchtrup and M. Torrilhon, Phys. Fluids **15**, 2668–2680 (2003).
[10] H. Struchtrup, Phys. Fluids **16**, 3921–3934 (2004).
[11] X. J. Gu and D. R. Emerson, J. Fluid Mech. **636**, 177–216 (2009).
[12] Z. Cai, Y. Fan, and R. Li, Comm. Pure Appl. Math. **67**, 464–518 (2014).
[13] Y. Fan, J. Koellermeier, J. Li, R. Li, and M. Torrilhon, J. Stat. Phys. **162**, 457–486 (2016).

[14] J. Köllermeier, "Derivation and numerical solutionof hyperbolic moment equationsfor rarefied gas flows," Ph.D. thesis, RWTH Aachen University, Germany 2017.
[15] H. Struchtrup and W. Weiss, Continuum Mech. Thermodyn. **12**, 1–18 (2000).
[16] M. Torrilhon and H. Struchtrup, J. Fluid Mech. **513**, 171–198 (2004).
[17] P. Taheri and H. Struchtrup, Phys. Rev. E **80**, p. 066317 (2009).
[18] P. Taheri, H. Struchtrup, and M. Torrilhon, Phys. Fluids **21**, p. 017102 (2009).
[19] P. Taheri, A. S. Rana, M. Torrilhon, and H. Struchtrup, Continuum Mech. Thermodyn. **21**, 423–443 (2009).
[20] A. Rana, M. Torrilhon, and H. Struchtrup, J. Comput. Phys. **236**, 169–186 (2013).
[21] A. S. Rana, A. Mohammadzadeh, and H. Struchtrup, Continuum Mech. Thermodyn. **27**, 433–446 (2015).
[22] V. K. Gupta and M. Torrilhon, Proc. Roy. Soc. A **471**, p. 20140754 (2015).
[23] V. K. Gupta, "Mathematical modeling of rarefied gas mixtures," Ph.D. thesis, RWTH Aachen University, Germany 2015.
[24] V. K. Gupta, H. Struchtrup, and M. Torrilhon, Phys. Fluids **28**, p. 042003 (2016).
[25] G. M. Kremer and W. Marques Jr., Kinet. Relat. Models **4**, 317–331 (2011).
[26] V. K. Gupta and P. Shukla, Indian Acad. Sci. Conf. Ser. **1**, 133–143 (2017).
[27] V. K. Gupta, P. Shukla, and M. Torrilhon, J. Fluid Mech. **836**, 451–501 (2018).
[28] V. K. Gupta and M. Torrilhon, AIP Conf. Proc. **1501**, 67–74 (2012).
[29] V. K. Gupta and M. Torrilhon, Comput. Math. Appl. **70**, 73–88 (2015).
[30] V. K. Gupta and M. Torrilhon, Comput. Math. Appl. **72**, 271–287 (2016).
[31] V. K. Gupta and M. Torrilhon, Automated Boltzmann collision integrals, https://web.mathcces.rwth-aachen.de/CollisionIntegrals (2012).
[32] E. P. Gross and S. Ziering, Phys. Fluids **2**, 701–712 (1959).
[33] M. L. Lavin and J. K. Haviland, Phys. Fluids **5**, 274–279 (1962).
[34] K. Frankowski, Z. Alterman, and C. L. Pekeris, Phys. Fluids **8**, 245–258 (1965).
[35] P. Bassanini, C. Cercignani, and C. Pagani, Int. J. Heat Mass Tran. **10**, 447–460 (1967).
[36] T. Ohwada, K. Aoki, and S. Yoshio, in *Rarefied Gas Dynamics: Theoretical and Computational Techniques* (AIAA, Washington, DC, 1989), pp. 70–81.
[37] T. Ohwada, Phys. Fluids **8**, 2153–2160 (1996).
[38] C. E. Siewert, J. Comput. Phys. **152**, 251–263 (1999).
[39] B.-T. Yeh and A. Frohn, Phys. Fluids **16**, 330–332 (1973).
[40] S. Kosuge, K. Aoki, and S. Takata, AIP Conf. Proc. **585**, 289–296 (2001).
[41] R. D. M. Garcia and C. E. Siewert, Phys. Fluids **16**, 3393–3402 (2004).
[42] R. D. M. Garcia and C. E. Siewert, Phys. Fluids **19**, p. 027102 (2007).
[43] A. Raines, Comput. Math. Math. Phys. **48**, 306–313 (2008).
[44] E. Barbera and F. Brini, Acta Mech. **220**, 87–105 (2011).
[45] J. L. Strapasson and F. Sharipov, Int. J. Heat Mass Tran. **71**, 91–97 (2014).
[46] F. J. McCormack, Phys. Fluids **16**, 2095–2105 (1973).
[47] J. C. Maxwell, Phil. Trans. R. Soc. Lond. **170**, 231–256 (1879).
[48] J. Kestin, K. Knierim, E. A. Mason, B. Najafi, S. T. Ro, and M. Waldman, J. Phys. Chem. Ref. Data **13**, 229–303 (1984).